Measurements of the top quark mass with the D0 detector

Oleg Brandt (for the D0 Collaboration)

Kirchhoff Institut für Physik, University of Heidelberg

FERMILAB-CONF-14-390-E

Abstract

The mass of the top quark is a fundamental parameter of the standard model (SM) and has to be determined experimentally. In this talk, I present the most recent measurements of the top quark mass in $p\bar{p}$ collisions at $\sqrt{s}$ = 1.96 TeV recorded by the D0 experiment at the Fermilab Tevatron Collider. The measurements are performed in final states containing two leptons, using 5.4 fb^{-1} of integrated luminosity, and one lepton, using 9.7 fb^{-1} of integrated luminosity. The latter constitutes the most precise single measurement of the mass of the top quark, corresponding to a relative precision of 0.43%. I conclude with a combination of our results with the results by the CDF collaboration, attaining a relative precision of 0.37%.

Keywords:
top quark, top quark mass, D0, Fermilab, matrix element, low-discrepancy sequences

1. Introduction

Since its discovery [1, 2], the determination of the properties of the top quark has been one of the main goals of the Fermilab Tevatron Collider, recently joined by the CERN Large Hadron Collider. The measurement of the top quark mass m_t, a fundamental parameter of the standard model (SM), has received particular attention. Indeed, m_t, the mass of the W boson M_W, and the mass of the Higgs boson are related through radiative corrections that provide an internal consistency check of the SM [3]. Furthermore, m_t dominantly affects the stability of the SM Higgs potential, which has related cosmological implications [4, 5, 6]. Currently, with m_t = 173.34 ± 0.76 GeV, a world-average combined precision of about 0.5% has been achieved [7, 8, 9].

Measurements of properties of the top quark other than m_t at D0 are reviewed in Ref. [10]. The full listing of top quark measurements at D0 can be found in Refs. [11].

At the Tevatron, top quarks are mostly pro duced in pairs via the strong interaction. By the end of Tevatron operation, about 10fb^{-1} of integrated luminosity were recorded by D0, which corresponds to about 80k produced $t\bar{t}$ pairs. In the framework of the SM, the top quark decays to a W boson and a b quark nearly 100% of the time, resulting in a $W^+W^-b\bar{b}$ final state from top quark pair production. Thus, $t\bar{t}$ events are classified according to the W boson decay channels as "dileptonic", "all–jets", or "lepton+jets".

2. Measurement of the top quark mass in dilepton final states

The most precise determination of m_t in dilepton final states at the Tevatron is performed by D0 using 5.4 fb^{-1} of data [12]. It is a combination of two measurements, using the matrix element (ME) technique [13], which will be described in Sec. 3 in the context of the ℓ + jets channel, and the neutrino weighting technique [12]. Leaving m_t as a free parameter, dilepton final states are

kinematically underconstrained by two degrees of freedom. To account for this in the analysis using ME, a prior is assumed for the transverse momentum distribution of the $t\bar{t}$ system, and the neutrino momenta are integrated over. In the neutrino weighting analysis, distributions in rapidities of the neutrino and the antineutrino are postulated, and a weight is calculated, which depends on the consistency of the reconstructed $\vec{p}_{\mathrm{T}}^{\nu\bar{\nu}} \equiv \vec{p}_{\mathrm{T}}^{\nu} + \vec{p}_{\mathrm{T}}^{\bar{\nu}}$ with the measured missing transverse momentum $\not{p}_{\mathrm{T}}$ vector, versus m_t. D0 uses the first and second moment of this weight distribution to define templates and extract m_t. To reduce the systematic uncertainty, the *in situ* JES calibration in ℓ+jets final states derived in Ref. [14] is applied, accounting for differences in jet multiplicity, luminosity, and detector ageing. A combination of both analyses in the dilepton final states at D0 yields $m_t = 173.9 \pm 1.9$ (stat) $\pm$ 1.6 (syst) GeV.

3. Measurement of the top quark mass in lepton+jets final states

The most precise measurement of m_t at D0 is performed in ℓ + jets final state with a matrix element (ME) technique, which determines the probability of observing each event under both the $t\bar{t}$ signal and background hypotheses described by the respective MEs [15]. The overall jet energy scale (JES) is calibrated *in situ* by constraining the reconstructed invariant mass of the hadronically decaying W boson to $M_W = 80.4$ GeV [16]. The measurement is performed using the full set of $p\bar{p}$ collision data at $\sqrt{s} = 1.96$ TeV recorded by the D0 detector in the Run II of the Fermilab Tevatron Collider, corresponding to an integrated luminosity of 9.7 fb^{-1}. In the present measurement, we not only use a larger data sample to improve the statistical precision, but also refine the estimation of systematic uncertainties through an updated detector calibration, in particular improvements to the b-quark JES corrections [17], and using recent improvements in modeling the $t\bar{t}$ signal. The analysis was performed blinded in m_t.

This analysis requires the presence of one isolated electron or muon with transverse momentum $p_{\mathrm{T}} > 20$ GeV and $|\eta| < 1.1$ or $|\eta| < 2$, respectively. In addition, exactly four jets with $p_{\mathrm{T}} > 20$ GeV within $|\eta| < 2.5$, and $p_{\mathrm{T}} > 40$ GeV for the jet of highest p_{T}, are required. Jet energies are corrected to the particle level using calibrations derived from exclusive γ+jet, Z+jet, and dijet events [17]. These calibrations account for differences in detector response to jets originating from a gluon, a b quark, and u, d, s, or c quarks. Furthermore, each event must have an imbalance in transverse momentum of $\not{p}_{\mathrm{T}} > 20$ GeV expected from the undetected neutrino. To further reduce background, at least one jet per event is required to be tagged as originating from a b quark (b-tagged).

The extraction of m_t is based on the kinematic information in the event and performed with a likelihood technique using per-event probability densities (PD) defined by the MEs of the processes contributing to the observed events. Assuming only two non-interfering contributing processes, $t\bar{t}$ and W + jets production, the per-event PD is:

$$\begin{aligned} P_{\mathrm{evt}} &= A(\vec{x})[f P_{\mathrm{sig}}(\vec{x}; m_t, k_{\mathrm{JES}}) \\ &+ (1-f) P_{\mathrm{bkg}}(\vec{x}; k_{\mathrm{JES}})] \,, \end{aligned} \tag{1}$$

where the observed signal fraction f, m_t, and the overall multiplicative factor adjusting the energies of jets after the JES calibration k_{JES}, are parameters to be determined from data. Here, $\vec{x}$ represents the measured jet and lepton four-momenta, and $A(\vec{x})$ accounts for acceptance and efficiencies. The function P_{sig} describes the PD for $t\bar{t}$ production. Similarly, P_{bkg} describes the PD for W + jets production, which contributes 14% of the data in the e + jets and 20% in the μ + jets channels.

In general, the set $\vec{x}$ of measured quantities will not be identical to the set of corresponding partonic variables $\vec{y}$ because of finite detector resolution and parton hadronization. Their relationship is described by the transfer function $W(\vec{x}, \vec{y}, k_{\mathrm{JES}})$, where we assume that the jet and lepton angles are known perfectly. The densities P_{sig} and P_{bkg} are calculated through a convolution of the differential partonic cross section, $\mathrm{d}\sigma(\vec{y})$, with $W(\vec{x}, \vec{y}, k_{\mathrm{JES}})$ and the PDs for the initial-state partons, $f(q_i)$, where the q_i are the momenta of the colliding partons, by integrating over all possible parton states leading to $\vec{x}$:

$$\begin{aligned} P_{\mathrm{sig}} &= \frac{1}{\sigma_{\mathrm{obs}}^{t\bar{t}}(m_t, k_{\mathrm{JES}})} \int \sum \mathrm{d}\sigma(\vec{y}, m_t) \mathrm{d}\vec{q}_1 \mathrm{d}\vec{q}_2 \\ &\times f(\vec{q}_1) f(\vec{q}_2) W(\vec{x}, \vec{y}; k_{\mathrm{JES}}) \,. \end{aligned} \tag{2}$$

The sum in the integrand extends over all possible flavor combinations of the initial state partons. The longitudinal momentum parton density functions (PDFs), $f(q_{i,z})$, are taken from the CTEQ6L1 set [18], while the dependencies $f(q_{i,\mathrm{x}})$, $f(q_{i,\mathrm{y}})$ on transverse momenta are taken from PDs obtained from the PYTHIA simulation [19]. The factor $\sigma_{\mathrm{obs}}^{t\bar{t}}(m_t, k_{\mathrm{JES}})$, defined as the expected total $t\bar{t}$ cross section, ensures that $A(\vec{x}) P_{\mathrm{sig}}$ is normalized to unity. The differential cross section, $\mathrm{d}\sigma(\vec{y}, m_t)$, is calculated using the leading order (LO) ME for the process $q\bar{q} \to t\bar{t}$. The $M_W = 80.4$ GeV constraint for the *in-situ* JES calibration is imposed by integrating over W boson masses from a Breit-Wigner prior.

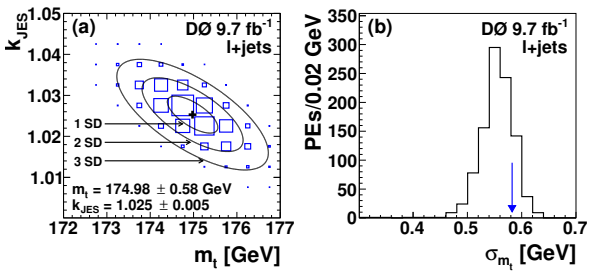

Figure 1: (color online) (a) Two-dimensional likelihood $\mathcal{L}(m_t, k_{\rm JES})/\mathcal{L}_{\rm max}$ for data. Fitted contours of equal probability are overlaid as solid lines. The maximum is marked with a cross. Note that the bin boundaries do not necessarily correspond to the grid points on which $\mathcal{L}$ is calculated. (b) Expected uncertainty distributions for m_t with the measured uncertainty indicated by the arrow.

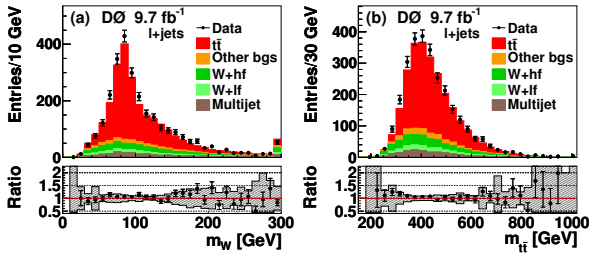

Figure 2: (color online) (a) Invariant mass of the jet pair matched to one of the W bosons. (b) Invariant mass of the $t\bar{t}$ system. In the ratio of data to SM prediction, the total systematic uncertainty is shown as a shaded band.

Source of uncertainty	Effect on m_t (GeV)
Signal and background modeling:	
Higher order corrections	+0.15
Initial/final state radiation	±0.09
Hadronization and UE	+0.26
Color reconnection	+0.10
Multiple $p\bar{p}$ interactions	−0.06
Heavy flavor scale factor	±0.06
b-jet modeling	+0.09
PDF uncertainty	±0.11
Detector modeling:	
Residual jet energy scale	±0.21
Flavor-dependent response to jets	±0.16
b tagging	±0.10
Trigger	±0.01
Lepton momentum scale	±0.01
Jet energy resolution	±0.07
Jet ID efficiency	−0.01
Method:	
Modeling of multijet events	+0.04
Signal fraction	±0.08
MC calibration	±0.07
Total systematic uncertainty	±0.49
Total statistical uncertainty	±0.58
Total uncertainty	±0.76

Table 1: Summary of uncertainties on the measured top quark mass. The signs indicate the direction of the change in m_t when replacing the default by the alternative model.

The density $P_{\rm sig}$ is calculated by numerical Monte Carlo (MC) integration. For this, we utilize the Sobol low discrepancy sequence [20] instead of pseudo-random numbers. This provides a reduction of about one order of magnitude in calculation time. Furthermore, we approximate the exact results of Eq. (2) for a grid of points in $(m_t, k_{\rm JES})$ space by calculating the ME only once for each m_t and multiplying the results with the transfer function $W(\vec{x}, \vec{y}; k_{\rm JES})$ to obtain $P_{\rm sig}$ for any $k_{\rm JES}$. This results in another order of magnitude reduction in computation time. Both improvements proved essential to reduce the statistical uncertainty in evaluating most of the systematic uncertainties discussed below.

The differential partonic cross section for $P_{\rm bkg}$ is calculated using the LO W + 4 jets MEs implemented in VECBOS [21]. The initial-state partons are all assumed to have zero transverse momentum $p_{\rm T}$.

Simulations are used to calibrate the ME technique. Signal $t\bar{t}$ events, as well as the dominant background contribution from W + jets production, are generated with ALPGEN [22] interfaced to PYTHIA. Therefore, it is the value of m_t as defined in the MC generator that is measured, and this value is expected to correspond within $\approx$ 1 GeV to m_t as defined in the pole mass scheme [23]. The detector response is fully simulated through GEANT3 [24], followed by the same reconstruction algorithms as used on data.

Seven samples of $t\bar{t}$ events, five at $m_t^{\rm gen} = 165, 170, 172.5, 175, 180$ GeV for $k_{\rm JES}^{\rm gen} = 1$, and two at $k_{\rm JES}^{\rm gen} = 0.95, 1.05$ for $m_t^{\rm gen} = 172.5$ GeV, are generated. Three samples of W + jets events, at $k_{\rm JES}^{\rm gen} = 0.95, 1$, and 1.05, are produced. Together, the $t\bar{t}$, W + jets and MJ samples are used to derive a linear calibration for the response of the ME technique to m_t and $k_{\rm JES}$. For each generated $(m_t^{\rm gen}, k_{\rm JES}^{\rm gen})$ point, 1000 pseudo-experiments (PE) are constructed, each containing the same number of events as observed in data.

Applying the ME technique to data, we measure after all calibrations $m_t = 174.98 \pm 0.58$ GeV and $k_{\rm JES} = 1.025 \pm 0.005$, where the total statistical uncertainty on m_t also includes the statistical contribution from $k_{\rm JES}$. Splitting the total statistical uncer-

tainty into two parts from m_t alone and $k_{\rm JES}$, we obtain $m_t = 174.98 \pm 0.41\,(\text{stat}) \pm 0.41\,(\text{JES})$ GeV. The two-dimensional likelihood distribution in $(m_t, k_{\rm JES})$ is shown in Fig. 1(a). Figure 1(b) compares the measured total statistical uncertainty on m_t with the distribution of this quantity from the PEs at $m_t^{\rm gen} = 172.5$ GeV and $k_{\rm JES}^{\rm gen} = 1$.

Comparisons of SM predictions to data for $m_t = 175$ GeV and $k_{\rm JES} = 1.025$ are shown in Fig. 2 for the invariant mass of the jet pair matched to one of the W bosons and the invariant mass of the $t\bar{t}$ system.

Systematic uncertainties are evaluated using PEs constructed from simulated signal and background events, for three categories: modeling of signal and background events, uncertainties in the simulation of the detector response, and uncertainties associated with procedures used and assumptions made in the analysis. Contributions from these sources are listed in Table 1.

The dominant category of systematic uncertainty is the modeling of signal events, with the largest contribution from *hadronisation and underlying event (UE)*, which is evaluated by comparing events simulated with ALPGEN interfaced to either PYTHIA or HERWIG. The JES calibration is derived using PYTHIA with a modified tune A [17], and is expected to be valid for this configuration only. Applying it to events that use HERWIG for evolving parton showers can lead to a sizable effect on m_t. However, this effect would not be present if the JES calibration were based on HERWIG. To avoid such double-counting of uncertainty sources, we evaluate the uncertainty from hadronization and UE by considering as $\vec{x}$ the momenta of particle level jets matched in (η, ϕ) space to reconstructed jets. In this evaluation, we reweight our default $t\bar{t}$ simulations in $p_{\rm T}^{t\bar{t}}$ to match ALPGEN interfaced to HERWIG. Another important contribution to the systematic uncertainty is from *higher order corrections*, which is evaluated by comparing events simulated with MC@NLO [25] to ALPGEN interfaced to HERWIG [26]. The uncertainty from the modeling of *initial and final state radiation* is constrained from Drell-Yan events [27]. As indicated by these studies, we change the amount of radiation via the renormalization scale parameter for the matching scale in ALPGEN interfaced to PYTHIA [28] up and down by a factor of 1.5. In addition, we reweight $t\bar{t}$ simulations in $p_{\rm T}$ of the $t\bar{t}$ system ($p_{\rm T}^{t\bar{t}}$) to match data, and combine the two effects in quadrature.

The category of systematic uncertainty from modeling of the detector response is dominated by the *residual jet energy scale* uncertainty from a potential dependence of the JES on $(p_{\rm T}, \eta)$. Its impact on m_t is estimated by changing the jet momenta as a function of $(p_{\rm T}, \eta)$ by the upper limits of JES uncertainty, the lower limits of JES uncertainty, and a linear fit within the limits of JES uncertainty. The maximum excursion in m_t is quoted as systematic uncertainty. Dedicated calibrations to account for the *flavour-dependent response* to jets originating from a gluon, a b quark and u, d, c, or s quarks are now an integral part of the JES correction [17], and the uncertainty on m_t from these calibrations is evaluated by changing them within their respective uncertainties. This systematic uncertainty accounts for the difference in detector response to b- and light-quark jets.

In summary, we measure

$$m_t = 174.98 \pm 0.58\,(\text{stat} + \text{JES}) \pm 0.49\,(\text{syst})\ \text{GeV}$$

with the ME technique in ℓ + jets final states, which is consistent with the values given by the current Tevatron and world combinations of the top quark mass [8, 9] and achieves by itself a similar precision. With an uncertainty of 0.43%, it constitutes the most precise single measurement of m_t.

4. Tevatron combination and outlook

Our results are included in the Tevatron combination from July 2014 [8], which is performed taking into account 10 published and 2 preliminary results from the CDF and D0 collaborations using $p\bar{p}$ collision data from Run I and Run II of the Fermilab Tevatron Collider. Taking into account potential correlations between considered sources of systematic uncertainty as described in great detail in Ref. [7], the final result reads $m_t = 174.34 \pm 0.64$ GeV corresponding to a precision of 0.37%, with a relative contribution from our measurement in ℓ+jets final states of 67%. An overview of input measurements performed using Run II data is presented in Fig. 3. The consistency of the input measurements is given by the value of the χ^2 distribution for 11 degrees of freedom and corresponds to a χ^2 probability of 46%.

Acknowledgments

I would like to thank my collaborators from the D0 experiment for their help in preparing this article. I also thank the staffs at Fermilab and collaborating institutions, as well as the D0 funding agencies.

References

[1] S. Abachi *et al.* (D0 Collaboration), Phys. Rev. Lett. **74**, 2632 (1995).
[2] F. Abe *et al.* (CDF Collaboration), Phys. Rev. Lett. **74**, 2626 (1995).

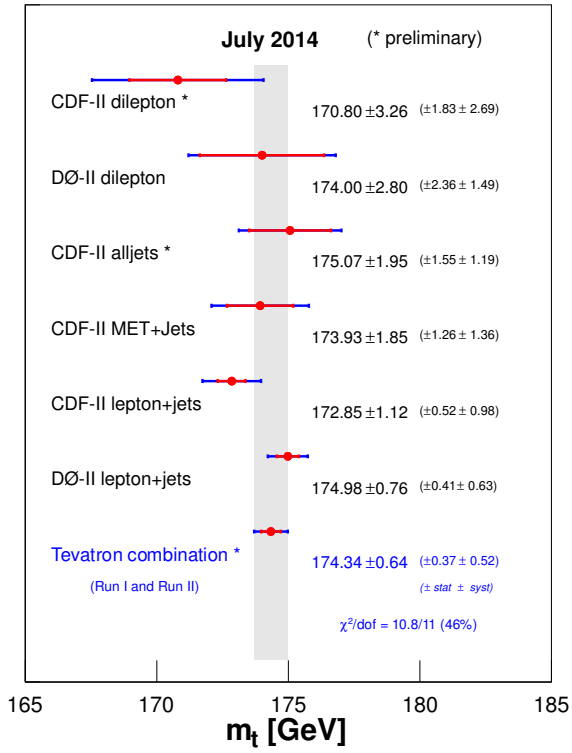

Figure 3: Summary of the measurements performed in Run II at the Tevatron which are used as inputs to the Tevatron combination [8]. The inner uncertainty bars in red indicate the statistical uncertainty, while the outer uncertainty bars in blue represent the total uncertainty. The Tevatron average value of m_t obtained using input measurements from Run I and Run II is given at the bottom, and its uncertainty is shown as a gray band. The Figure is adapted from Ref. [8].

[3] The ALEPH, CDF, D0, DELPHI, L3, OPAL, SLC Collaborations, the LEP Electroweak Working Group, the Tevatron Electroweak Working Group, and the SLD electroweak and heavy flavour groups, arXiv:hep-ex/1012.2367; LEP Electroweak Working Group, `http://lepewwg.web.cern.ch/LEPEWWG/`.

[4] G. Degrassi *et al.*, J. High Energy Phys. 08 (2012) 098.

[5] F. Bezrukov *et al.*, Phys. Lett. B **659**, 703 (2008).

[6] A. De Simone *et al.*, Phys. Lett. B **678**, 1 (2009).

[7] T. Aaltonen *et al.* (CDF and D0 Collaborations), Phys. Rev. D **86**, 092003 (2012) and references therein.

[8] T. Aaltonen *et al.* (CDF and D0 Collaborations), arXiv:1407.2682 [hep-ex] (2014) and references therein.

[9] G. Aad *et al.* (ATLAS, CDF, CMS, and D0 Collaborations), arXiv:1403.4427 [hep-ex] (2014) and references therein.

[10] C. Schwanenberger, these proceedings; R. Demina, these proceedings.

[11] `http://www-d0.fnal.gov/Run2Physics/WWW/results/top.htm`, `http://www-d0.fnal.gov/Run2Physics/WWW/documents/Run2Results.htm`

[12] V. M. Abazov *et al.* (D0 Collaboration), Phys. Rev. D 86, 051103(R) (2012).

[13] V. M. Abazov *et al.* (D0 Collaboration), Phys. Rev. Lett. 107, 082004 (2011).

[14] V. M. Abazov *et al.* (D0 Coll.), Phys. Rev. D **84**, 032004 (2011).

[15] V. M. Abazov *et al.* (D0 Collaboration), Nature **429**, 638 (2004).

[16] T. Aaltonen *et al.* (CDF and D0 Collaborations), Phys. Rev. D **88**, 052018 (2013).

[17] V. M. Abazov *et al.* (D0 Collaboration), Nucl. Instrum. Methods Phys. Res. Sec. A, **763**, 442 (2014).

[18] J. Pumplin *et al.*, J. High Energy Phys. 07 (2002) 012.

[19] T. Sjöstrand *et al.*, Comp. Phys. Commun. **135**, 238 (2001); T. Sjöstrand, S. Mrenna, and P. Skands, J. High Energy Phys. 05 (2006) 026.

[20] I. M. Sobol, Zh. Vych. Mat. Fiz. **7** 784 (1967, in Russian); U.S.S.R Comput. Maths. Math. Phys. **7**, 86 (in English).

[21] F. A. Berends *et al.*, Nucl. Phys. B **357**, 32 (1991).

[22] M. L. Mangano *et al.*, J. High Energy Phys. 07 (2003) 001.

[23] J. Beringer *et al.* (Particle Data Group), Phys. Rev. D **86**, 010001 (2012).

[24] CERN Application Software Group, CERN Program Library Long Writeup W5013, CERN, Geneva (1993).

[25] S. Frixione and B. R. Webber, J. High Energy Phys. 06 (2002) 029.

[26] G. Corcella *et al.*, J. High Energy Phys. 01 (2001) 010.

[27] V. M. Abazov *et al.* (D0 Collaboration) Phys. Rev. Lett. **106**, 122001 (2011).

[28] B. Cooper, J. Katzy, M. L. Mangano, A. Messina, L. Mijovic, and P. Skands, Eur. Phys. J. C **72**, 2078 (2012).